

Towards automation of operando experiments: A case study in contactless conductivity measurements

P. Kraus,* E. H. Wolf, C. Prinz, G. Bellini, A. Trunschke, and R. Schlögl

Supplementary Material

Table of contents

Examples of log files:

- | | |
|--|-------|
| 1. Excerpt from an <i>instrument log</i> file. | p. S2 |
| 2. Excerpt from a <i>VNA log</i> file. | p. S3 |

Tabulated summary of the catalytic data:

- | | |
|--|-------|
| 3. Summary of the MCPT data for samples activated in C ₃ -oxidation, studied with the <i>Handbook</i> protocol. The full archive, including <i>datagrams</i> , <i>schema</i> files, <i>parameter files</i> , and all raw data, is available at DOI: 10.5281/zenodo.5008960 | p. S4 |
| 4. Summary of the MCPT data for other samples studied with the <i>Handbook</i> protocol. The full archive, including <i>datagrams</i> , <i>schema</i> files, <i>parameter files</i> , and all raw data, is available at DOI: 10.5281/zenodo.5010992 | p. S4 |
| 5. Summary of the MCPT data for samples studied with the perovskite protocol. The full archive, including <i>datagrams</i> , <i>schema</i> files, <i>parameter files</i> , and all raw data, is available at DOI: 10.5281/zenodo.4980210 | p. S5 |

Overview of the MCPT instrument:

- | | |
|--|-------|
| 6. Simplified block diagram of the MCPT instrument | p. S7 |
| 7. A list of key instrument components | p. S7 |
| 8. Piping and instrumentation diagram of the MCPT instrument | p. S8 |

*E-Mail: peter.kraus@curtin.edu.au

Detailed description of instrument components:

9. Microwave cavities	p. S9
10. Custom glassware	p. S10
11. Temperature controller	p. S14
12. Transmission line	p. S16

Additional supplemental files and archives in computer-readable form are available on Zenodo, see DOI: [10.5281/zenodo.5011202](https://doi.org/10.5281/zenodo.5011202). An executable version of this archive is available on [Binder](#).

```

1 timestamp; elapsed; T_f; T_fs; T_fo; T_c; T_cs; T_co; N2; O2; alkane; CO/CO2; sat.; press.; flow low; flow high; cav. flush; heater flow; T_cal
2 ; C; %; C; %; ml/min; ml/min; ml/min; mbar; ml/min; ml/min; l/min; C
3 2019-08-29-16-36-37; 0h 1m 0s; 22.9; 21.6; 0.0; 18; 18; -12; 28.12; 1.48; 0.00; 0.00; 0.00; 1300.6; 1.210; 0.00; 15; 8; 20.6
4 2019-08-29-16-37-37; 0h 2m 0s; 22.9; 23.6; 1.3; 18; 18; -6; 28.12; 1.48; 0.00; 0.00; 0.00; 1299.7; 1.210; 0.00; 15; 8; 21.0
5 2019-08-29-16-38-38; 0h 3m 1s; 23.1; 25.6; 9.3; 18; 18; -11; 28.12; 1.48; 0.00; 0.00; 0.00; 1299.4; 1.209; 0.00; 15; 8; 20.5
6 2019-08-29-16-39-39; 0h 4m 2s; 26.0; 27.7; 11.8; 18; 18; -12; 28.12; 1.48; 0.00; 0.00; 0.00; 1300.3; 1.211; 0.00; 15; 8; 21.0
7 2019-08-29-16-40-39; 0h 5m 2s; 29.0; 29.7; 12.1; 18; 18; -18; 28.13; 1.48; 0.00; 0.00; 0.00; 1300.0; 1.210; 0.00; 15; 8; 20.3
8 2019-08-29-16-41-40; 0h 6m 3s; 31.1; 31.7; 13.0; 18; 18; -8; 28.11; 1.48; 0.00; 0.00; 0.00; 1299.7; 1.210; 0.00; 15; 8; 20.1
9 2019-08-29-16-42-40; 0h 7m 3s; 33.1; 33.7; 13.9; 18; 18; -10; 28.12; 1.48; 0.00; 0.00; 0.00; 1300.0; 1.211; 0.00; 15; 8; 20.3
10 2019-08-29-16-43-40; 0h 8m 4s; 35.1; 35.7; 14.7; 18; 18; -12; 28.12; 1.48; 0.00; 0.00; 0.00; 1299.7; 1.210; 0.00; 15; 8; 20.3
11 2019-08-29-16-44-41; 0h 9m 4s; 37.2; 37.7; 15.4; 18; 18; -2; 28.12; 1.48; 0.00; 0.00; 0.00; 1299.4; 1.212; 0.00; 15; 8; 20.9
12 2019-08-29-16-45-41; 0h 10m 5s; 39.2; 39.7; 16.1; 18; 18; -17; 28.12; 1.48; 0.00; 0.00; 0.00; 1299.7; 1.210; 0.00; 15; 8; 21.9
13 [...]
14 2019-08-29-18-46-08; 2h10m32s; 252.0; 252.0; 48.6; 18; 18; -7; 28.11; 1.48; 0.00; 0.00; 0.00; 1300.0; 1.211; 0.00; 15; 8; 20.2
15 2019-08-29-18-47-09; 2h11m32s; 252.0; 252.0; 48.7; 18; 18; -20; 28.12; 1.48; 0.00; 0.00; 0.00; 1300.6; 1.211; 0.00; 15; 8; 20.2
16 2019-08-29-18-48-09; 2h12m32s; 252.0; 252.0; 48.8; 18; 18; -22; 28.12; 1.48; 0.00; 0.00; 0.00; 1300.6; 1.211; 0.00; 15; 8; 20.2
17 2019-08-29-18-49-10; 2h13m33s; 252.0; 252.0; 48.5; 18; 18; -17; 28.12; 1.48; 0.00; 0.00; 0.00; 1300.0; 1.212; 0.00; 15; 8; 20.7
18 2019-08-29-18-50-11; 2h14m34s; 252.0; 252.0; 48.8; 18; 18; -19; 28.12; 1.48; 0.00; 0.00; 0.00; 1300.0; 1.211; 0.00; 15; 8; 20.6
19 2019-08-29-18-51-11; 2h15m34s; 252.3; 252.8; 49.7; 18; 18; -18; 28.12; 1.3; 3.32; 7.32; 0.00; 0.00; 1300.0; 0.653; 0.95; 15; 8; 20.6
20 2019-08-29-18-52-12; 2h16m36s; 254.4; 254.8; 49.3; 18; 18; -16; 28.12; 1.3; 3.32; 7.33; 0.00; 0.00; 1300.6; 0.656; 0.98; 15; 8; 20.8
21 2019-08-29-18-53-13; 2h17m37s; 256.4; 256.8; 49.8; 18; 18; -20; 28.12; 1.3; 3.32; 7.34; 0.00; 0.00; 1300.6; 0.656; 1.00; 15; 8; 20.1
22 2019-08-29-18-54-14; 2h18m37s; 258.5; 258.9; 49.9; 18; 18; -15; 28.12; 1.3; 3.32; 7.35; 0.00; 0.00; 1300.0; 0.656; 0.99; 15; 8; 19.9
23 2019-08-29-18-55-16; 2h19m39s; 260.5; 260.9; 50.3; 18; 18; -18; 28.12; 1.3; 3.32; 7.33; 0.00; 0.00; 1300.6; 0.656; 1.00; 15; 8; 19.8
24 [...]
25 2019-08-31-20-31-59; 51h56m22s; 423.0; 423.0; 68.3; 19; 18; -40; 28.12; 1.3; 3.32; 7.36; 0.00; 0.00; 1299.7; 0.656; 0.00; 15; 8; 21.5
26 2019-08-31-20-33-00; 51h57m23s; 423.0; 423.0; 68.4; 19; 18; -30; 28.12; 1.3; 3.32; 7.34; 0.00; 0.00; 1300.0; 0.657; 0.00; 15; 8; 21.5
27 2019-08-31-20-34-01; 51h58m24s; 423.0; 423.0; 68.2; 19; 18; -32; 28.12; 1.3; 3.32; 7.34; 0.00; 0.00; 1300.3; 0.656; 0.00; 15; 8; 21.6
28 2019-08-31-20-35-01; 51h59m25s; 423.0; 423.0; 68.2; 19; 18; -31; 28.12; 1.3; 3.32; 7.34; 0.00; 0.00; 1299.4; 0.656; 0.00; 15; 8; 20.9
29 2019-08-31-20-36-02; 52h 0m25s; 411.1; 20.0; 0.0; 19; 18; -29; 28.13; 1.65; 0.00; 0.00; 0.00; 1294.4; 1.260; 24.43; 15; 8; 21.2
30 2019-08-31-20-37-02; 52h 1m25s; 285.8; 20.0; 0.0; 19; 18; -32; 28.12; 1.48; 0.00; 0.00; 0.00; 1300.0; 1.211; 0.99; 15; 8; 21.1
31 2019-08-31-20-38-03; 52h 2m26s; 17.2.5; 20.0; 0.0; 18; 18; -12; 28.12; 1.48; 0.00; 0.00; 0.00; 1299.7; 1.210; 0.99; 15; 8; 21.3
32 2019-08-31-20-39-03; 52h 3m26s; 10.5.2; 20.0; 9.9; 18; 18; -20; 28.12; 1.48; 0.00; 0.00; 0.00; 1299.7; 1.211; 0.99; 15; 8; 21.6
33 2019-08-31-20-40-05; 52h 4m28s; 69.7; 20.0; 0.0; 18; 18; -17; 28.12; 1.48; 0.00; 0.00; 0.00; 1299.7; 1.211; 1.00; 15; 8; 21.8
34 2019-08-31-20-41-06; 52h 5m29s; 51.3; 20.0; 0.0; 18; 18; -17; 28.12; 1.48; 0.00; 0.00; 0.00; 1299.7; 1.211; 1.00; 15; 8; 20.9

```

Figure S1: Excerpt from an *instrument log* file, showing an example of start-up with a ramp reaching 252°C at 2°C/min (3-12), switch of feed from oxidative to reaction (14-23) and cooldown procedure (25-34). The header (highlighted in green) lists the columns, which correspond to the timestamp, elapsed run time, inlet temperature setpoint, heater duty cycle, cavity temperature, cavity pressure, inlet flow (meter no. 1), inlet flow (meter no. 2), cavity flush, heater medium flow, temperature of the calibration thermocouple.

```

1  BW = 10000;AVG = 10
2 +7.100000E+9 -2.280313E-2 +9.412804E-1
3 +7.100015E+9 -2.241943E-2 +9.409110E-1
4 +7.100030E+9 -2.244101E-2 +9.406135E-1
5 +7.100045E+9 -2.181034E-2 +9.407906E-1
6 +7.100060E+9 -2.154459E-2 +9.396642E-1
7 +7.100075E+9 -2.166180E-2 +9.403051E-1
8 +7.100090E+9 -2.122021E-2 +9.408551E-1
9 +7.100105E+9 -2.164769E-2 +9.408164E-1
10 +7.100120E+9 -2.139573E-2 +9.404883E-1
11 +7.100135E+9 -2.145294E-2 +9.407361E-1
12 [...]
13 +7.399865E+9 -2.219277E-2 -9.154096E-1
14 +7.399880E+9 -2.249969E-2 -9.151102E-1
15 +7.399895E+9 -2.282277E-2 -9.154791E-1
16 +7.399910E+9 -2.304419E-2 -9.154005E-1
17 +7.399925E+9 -2.431337E-2 -9.159150E-1
18 +7.399940E+9 -2.515590E-2 -9.163996E-1
19 +7.399955E+9 -2.466450E-2 -9.154912E-1
20 +7.399970E+9 -2.516757E-2 -9.149708E-1
21 +7.399985E+9 -2.563848E-2 -9.151121E-1
22 +7.400000E+9 -2.602740E-2 -9.156989E-1

```

Figure S2: Excerpt from a *VNA log* file. Only the header (highlighted in green) and the first and last 10 lines shown. The header lists the filter bandwidth (10000 Hz) and number of shots averaged (10). The columns correspond to the frequency f and the real and complex parts of the reflection coefficient $\Gamma(f)$.

Table S1: Results of the operando MCPT investigations of transition metal oxide samples, activated in C₃-oxidation, using the *Handbook* protocol. Columns include the name and nominal atomic composition, sample ID, reference conductivity at 300°C, activation energy of conductivity, changes in conductivity as a function of inlet stoichiometry and residence time, activation energy of mass-normalized conversion, the ideality of conversion with residence time, and interpolated selectivities to CO_x and C₃H₆ at 5% conversion (dashes correspond to cases where X is well below or above 5%).

Sample name	Sample ID	σ_r [S/m]	$E_A(\sigma)$ [kJ/mol]	$\Delta\sigma(\phi)$ [S/m]	$\Delta\sigma(\tau)$ [S/ms]	$E_A(X/m)$ [kJ/mol]	$\Delta X(\tau)/X$ [%]	S_{CO_x} (5%) [%]	$S_{C_3H_6}$ (5%) [%]
”VPP”-C ₃	32082	0.005(4)	20(1)	0.0067(7)	-0.00018(6)	16(31)	7(20)	99(5)	59(4)
MoO ₃ -C ₃	31845	0.02(1)	11(2)	0.00045(5)	0.0001(1)	76(15)	88(15)	-	-
MoVO _x -C ₃	31804	0.6(2)	9.43(4)	-0.00515(7)	-0.0042(1)	80(2)	90(4)	56.87(6)	18.6(1)
MoVTeNbO _x -C ₃	31821	0.33(8)	0.07(3)	0.0053(1)	0.00076(4)	86(2)	75(2)	39.9(1)	31.4(4)
Sm _{0.95} MnO ₃ -C ₃	31836	15(4)	5.21(6)	-0.009(2)	0.006(1)	62(3)	62(4)	88.3(1)	11.7(1)
V ₂ O ₅ -C ₃	31846	0.8(4)	8.03(4)	0.036(2)	0.0161(1)	66(15)	75(13)	69.61(5)	30.23(4)
VPP-C ₃	31849	0.03(1)	11.1(5)	-0.00117(8)	-0.00062(5)	66(6)	59(5)	78(1)	15.4(2)
VWPO _x -C ₃	31851	0.19(5)	17.8(2)	0.0069(1)	0.0021(1)	86(3)	87(3)	81.09(6)	17.92(7)
α -V _{0.8} W _{0.2} OP _{0.4} -C ₃	31850	0.14(4)	14.73(4)	0.00013(2)	0.00007(4)	86(4)	87(5)	69.89(9)	29.49(5)
α -VOPO ₄ -C ₃	32084	0.005(6)	43(3)	0.0081(3)	0.0017(2)	86(44)	88(47)	48.82(5)	50.62(6)
β -VOPO ₄ -C ₃	31848	0.021(7)	12.7(2)	0.00257(5)	0.00042(1)	80(11)	79(10)	42.50(5)	57.13(5)

Table S2: Results of the operando MCPT investigations of selected samples without previous activation in C₃-oxidation, using the *Handbook* protocol. Columns as in Table S1.

Sample name	Sample ID	σ_r [S/m]	$E_A(\sigma)$ [kJ/mol]	$\Delta\sigma(\phi)$ [S/m]	$\Delta\sigma(\tau)$ [S/ms]	$E_A(X/m)$ [kJ/mol]	$\Delta X(\tau)/X$ [%]	S_{CO_x} (5%) [%]	$S_{C_3H_6}$ (5%) [%]
LaMnO ₃	30649	11(4)	-0.54(3)	0.0037(9)	0.008(2)	69(3)	69(5)	91.5(1)	8.4(1)
MoVTeNbO _x	31652	0.5(2)	0.88(6)	0.0190(5)	0.0009(2)	90(7)	88(10)	38.10(7)	37.7(1)
PrMnO ₃	30650	1.8(5)	0.27(3)	-0.0021(3)	0.0019(3)	61(2)	56(3)	88.444(8)	11.47(2)
Sm _{0.95} MnO ₃	30869	18(6)	5.30(2)	-0.0086(8)	-0.003(2)	60(5)	62(7)	91.3(1)	8.6(1)
V ₂ O ₅	31034	0.5(2)	8.68(9)	-0.012(5)	0.0229(1)	60(5)	58(4)	77.4(2)	22.1(2)
silica gel	19760	0.017(4)	18(3)	-0.00002(3)	0.00002(6)	101(4)	78(4)	77.4(2)	16.6(2)

Table S3: Results of the operando MCPT investigations of copper-doped lanthanide manganates, using the perovskite protocol.
 Columns as in Table S1

Sample name	Sample ID	σ_r [S/m]	$E_A(\sigma)$ [kJ/mol]	$\Delta\sigma(\phi)$ [S/m]	$\Delta\sigma(\tau)$ [S/ms]	$E_A(X/m)$ [kJ/mol]	$\Delta X(\tau)/X$ [%]	$S_{CO_x}(5\%)$ [%]	$S_{C_3H_6}(5\%)$ [%]
LaMn _{0.60} Cu _{0.40} O ₃	31285	6(2)	10.02(8)	-0.15(1)	0.95(7)	72(3)	42(13)	79.88(4)	20.04(3)
LaMn _{0.65} Cu _{0.35} O ₃	30624	1.0(3)	13.7(2)	0.023(2)	0.61(8)	79(2)	41(7)	66.6(5)	33.5(4)
LaMn _{0.70} Cu _{0.30} O ₃	30659	1.9(5)	16.3(2)	0.0572(9)	0.91(7)	79(2)	50(10)	—	—
LaMn _{0.75} Cu _{0.25} O ₃	30635	1.4(4)	18.3(2)	0.043(1)	1.08(7)	75(2)	50(10)	75.44(5)	24.45(4)
LaMn _{0.80} Cu _{0.20} O ₃	31180	1.8(9)	9.71(8)	0.0100(8)	0.23(3)	81(11)	38(4)	28.9(6)	70.5(8)
LaMn _{0.90} Cu _{0.10} O ₃	30867	4(1)	13.6(1)	0.066(1)	0.97(7)	78(5)	40(19)	—	—
LaMnO ₃	30649	26(18)	5.79(8)	0.038(7)	2.6(2)	72(17)	47(68)	—	—
PrMn _{0.60} Cu _{0.40} O ₃	31163	2(1)	6.47(6)	-0.065(3)	0.27(2)	76(14)	35(55)	71.25(8)	28.65(5)
PrMn _{0.65} Cu _{0.35} O ₃	31176	2.7(8)	2.69(4)	0.020(1)	0.18(2)	73(3)	49(11)	74.1(2)	25.6(2)
PrMn _{0.70} Cu _{0.30} O ₃	30934	4(1)	5.02(7)	0.014(1)	0.66(5)	82(2)	43(10)	72.95(6)	26.83(5)
PrMn _{0.75} Cu _{0.25} O ₃	30637	2.6(9)	8.38(9)	0.0245(9)	0.66(5)	81(5)	34(21)	68(2)	32(2)
PrMn _{0.80} Cu _{0.20} O ₃	31021	3(1)	8.10(5)	0.0131(5)	0.32(3)	71(8)	43(32)	77(7)	23(7)
PrMn _{0.90} Cu _{0.10} O ₃	31070	10(3)	2.00(6)	0.014(3)	0.85(6)	65(4)	46(15)	68(2)	32(3)
PrMnO ₃	30650	1.8(5)	11.87(9)	0.0169(5)	0.32(3)	69(2)	25(8)	78(7)	22(7)

Diagrams and equipment list for the MCPT instrument

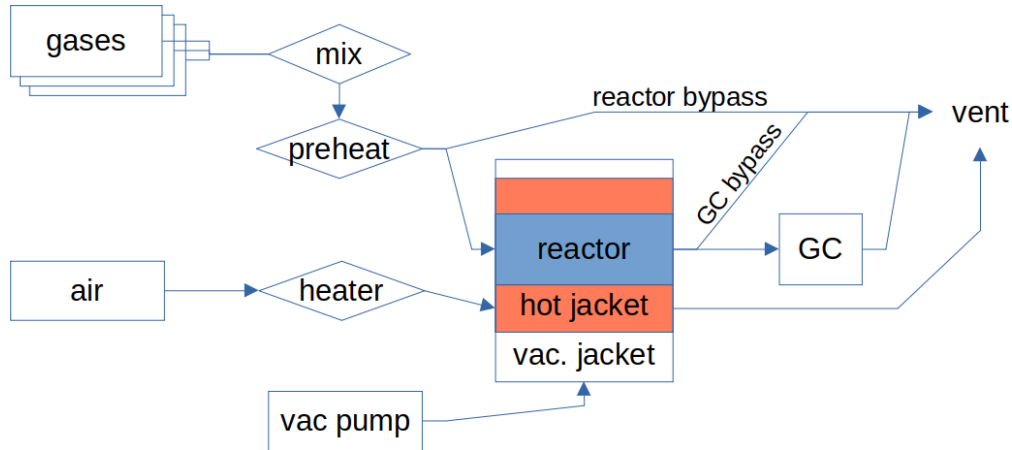


Figure S3: A simplified block diagram of the gas flows in the MCPT instrument. A more detailed overview is shown in the detailed piping & instrumentation diagram (P&ID) in Fig. S4. A schema of the cavity containing the reactor assembly is shown in Fig. S5. A list of the key components of the MCPT instrument is in Table S4

Table S4: List of key electronic components

P&ID label	P&ID position	Description	Model
FC	4B-5C	Mass flow controllers	Bronkhorst EL-FLOW Prestige †
PC	5B	Pressure controller	Bronkhorst EL-PRESS †
TR	5C	Temperature controller	Eurotherm 5304, see Figs. S11 and S12
—	5C	Heater	Serpentine III F017558, see Fig. S11
FI, Alarmbox	4C	Flow meter	SMC PFM 725, see Fig. S11
VNA	4D	Vector network analyser	Agilent PNA-L N5320C, see Fig. S13
GC	6D	Gas chromatograph	Agilent 7890 GC ‡
—	6B-6C	Vacuum pumps	Pfeiffer HiCube 80
PI	6B	Vacuum gauge	Pfeiffer PKR 251
—	6C-6E	Trace heating	Horst HSTD 200W *

† : Controlled using the LabVIEW interface, via a FlowBus controller (E-7500) and a set of three multiport adapters for a total of 10 devices on a single bus. Note: Only 7 devices shown in Fig. S4.

‡ : Equipped with two channels: 1) Plot-Molesieve (30 m length, 50 μm film thickness, 0.53 mm I.D.) into Plot-Q (30 m length, 40 μm film thickness, 0.53 mm I.D.) into a thermal conductivity detector; 2) FFAP (30 m length, 1 μm film thickness, 0.53 mm I.D.) into Plot-Q (30 m length, 40 μm film thickness, 0.53 mm I.D.) into a Polyarc detector (Activated Research Company). Online gas analysis using a 250 μl sampling loop (Vici Valco, SL250CW) and multi-port valves (Vici Valco, 2×DC6WE, 1×DC10WE).

* : Regulators built in-house.

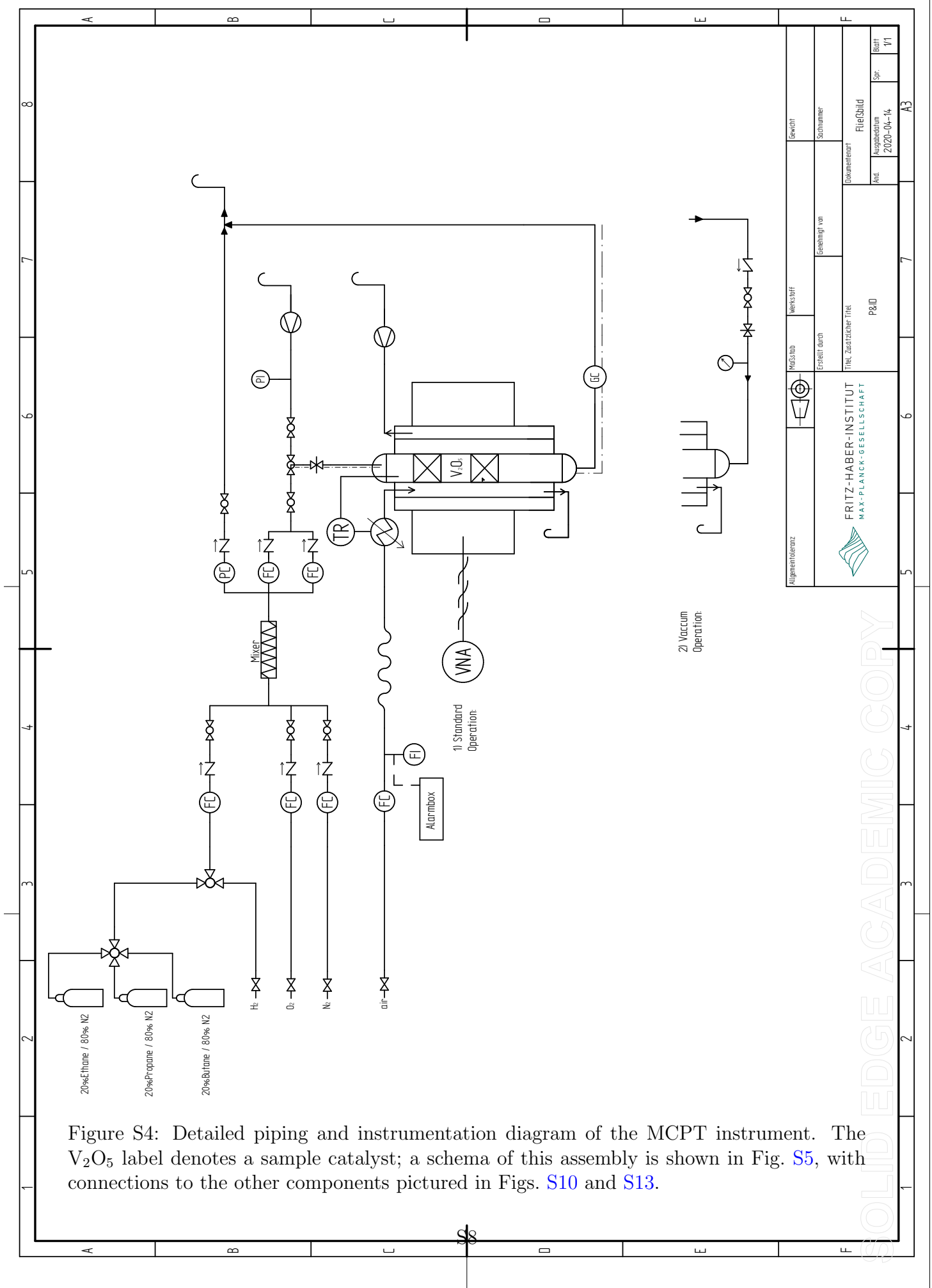


Figure S4: Detailed piping and instrumentation diagram of the MCPT instrument. The V₂O₅ label denotes a sample catalyst; a schema of this assembly is shown in Fig. S5, with connections to the other components pictured in Figs. S10 and S13.

Details of the cavities

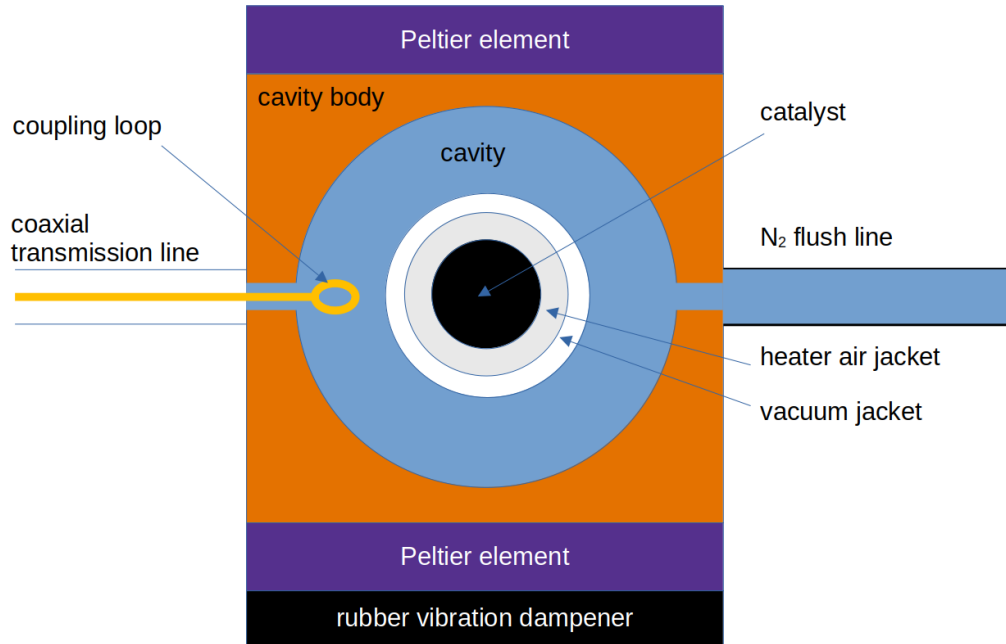


Figure S5: A schema of the cavity, glass dewar reactor assembly, coupling loop, and cooling (Peltier) elements. Not to scale.



Figure S6: A photo of MCPT cavities of various sizes, made from copper, plated with silver and gold. The disassembled cavity on the right ($h_c = 20$ mm, $r_c = 34$ mm) has been used throughout this work.

Details of the custom glassware and its connecting hardware

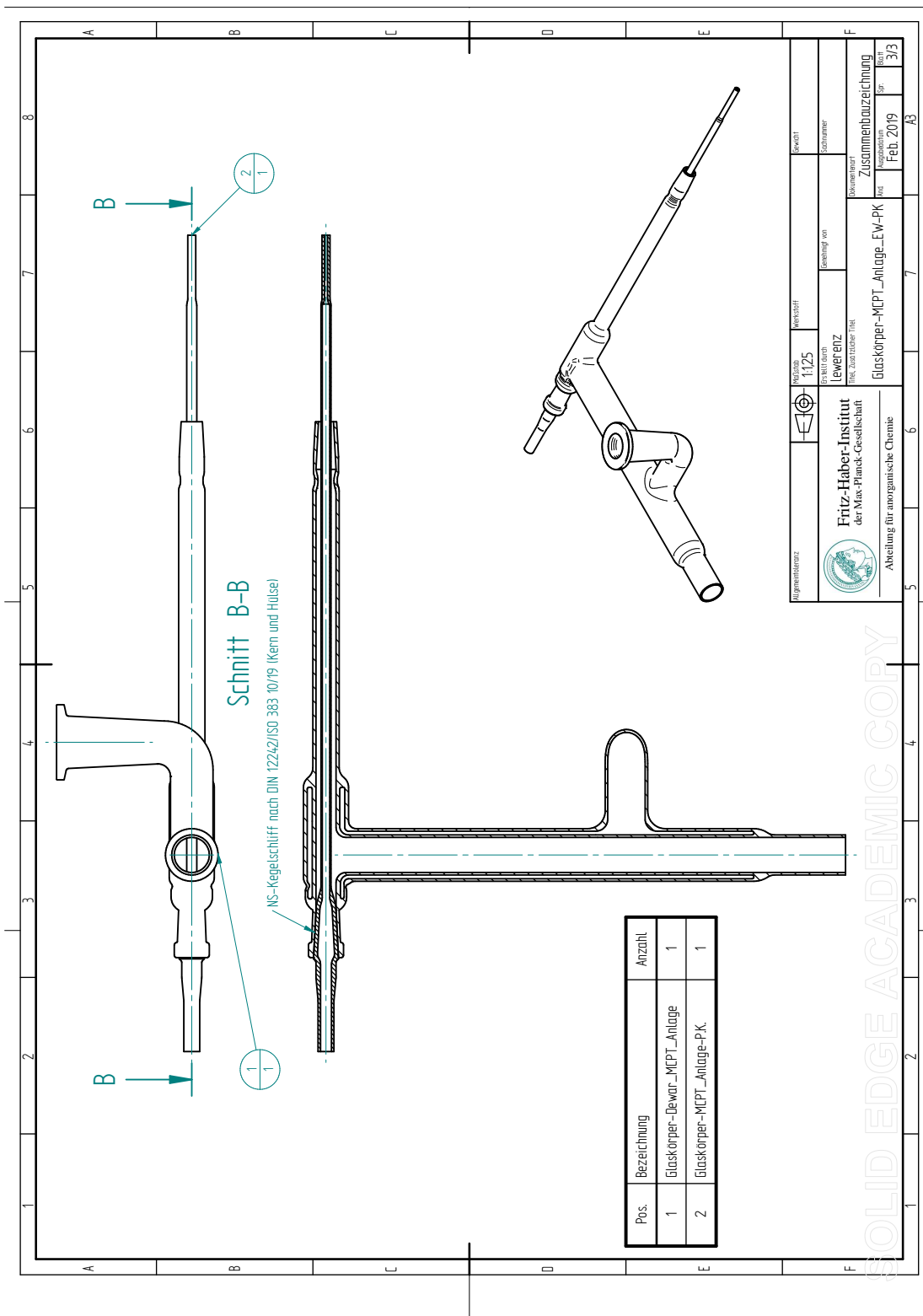


Figure S7: Complete glassware reactor assembly (Quarzglas Heinrich, Aachen). The dimensions of the reactors are shown in Fig. S8, while the dewar is shown in Fig. S9. The whole assembly is inserted into the cavity as indicated in Fig. S5.

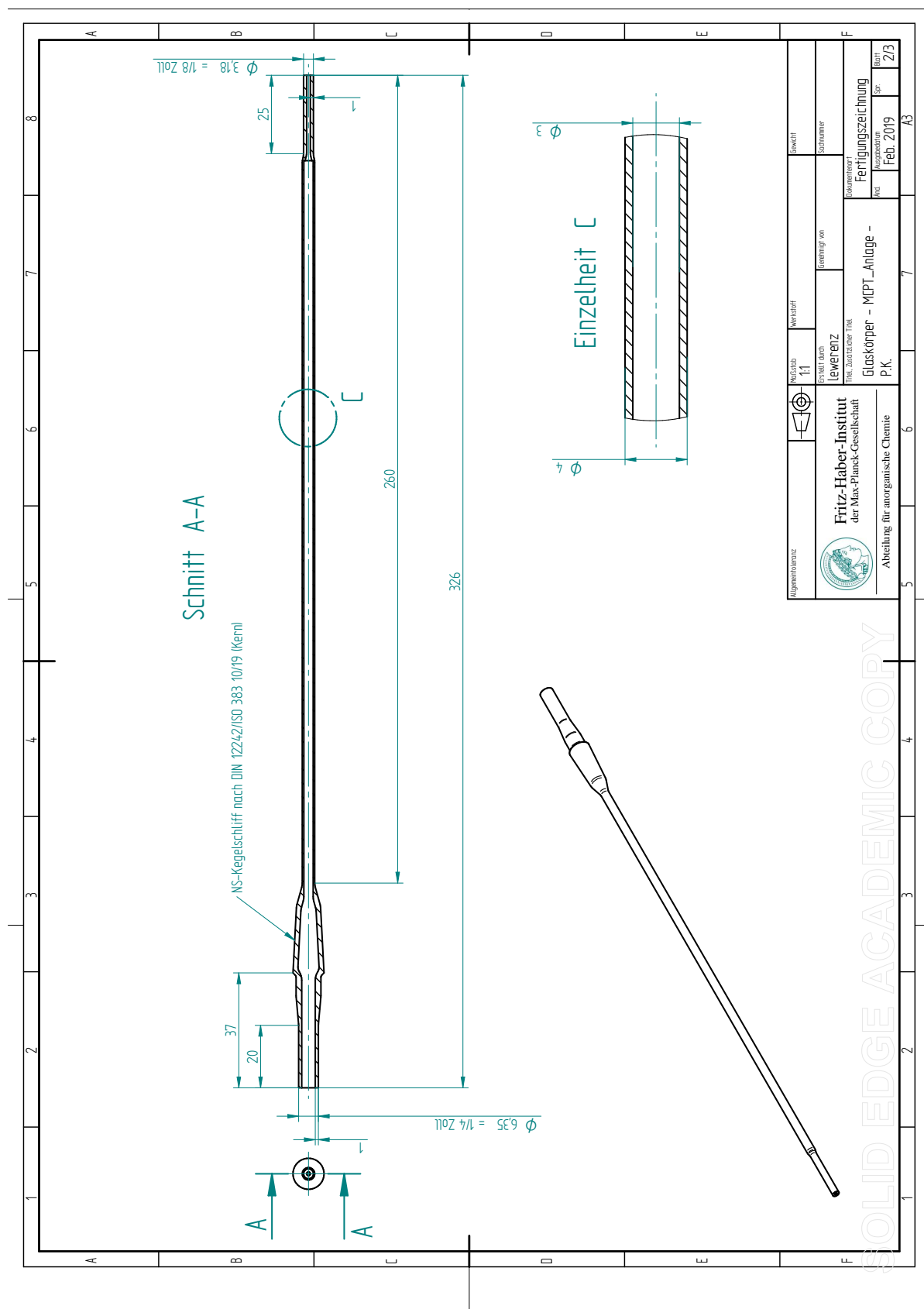


Figure S8: Catalytic reactor, made from Ilmasil PN (Quarzglas Heinrich, Aachen).

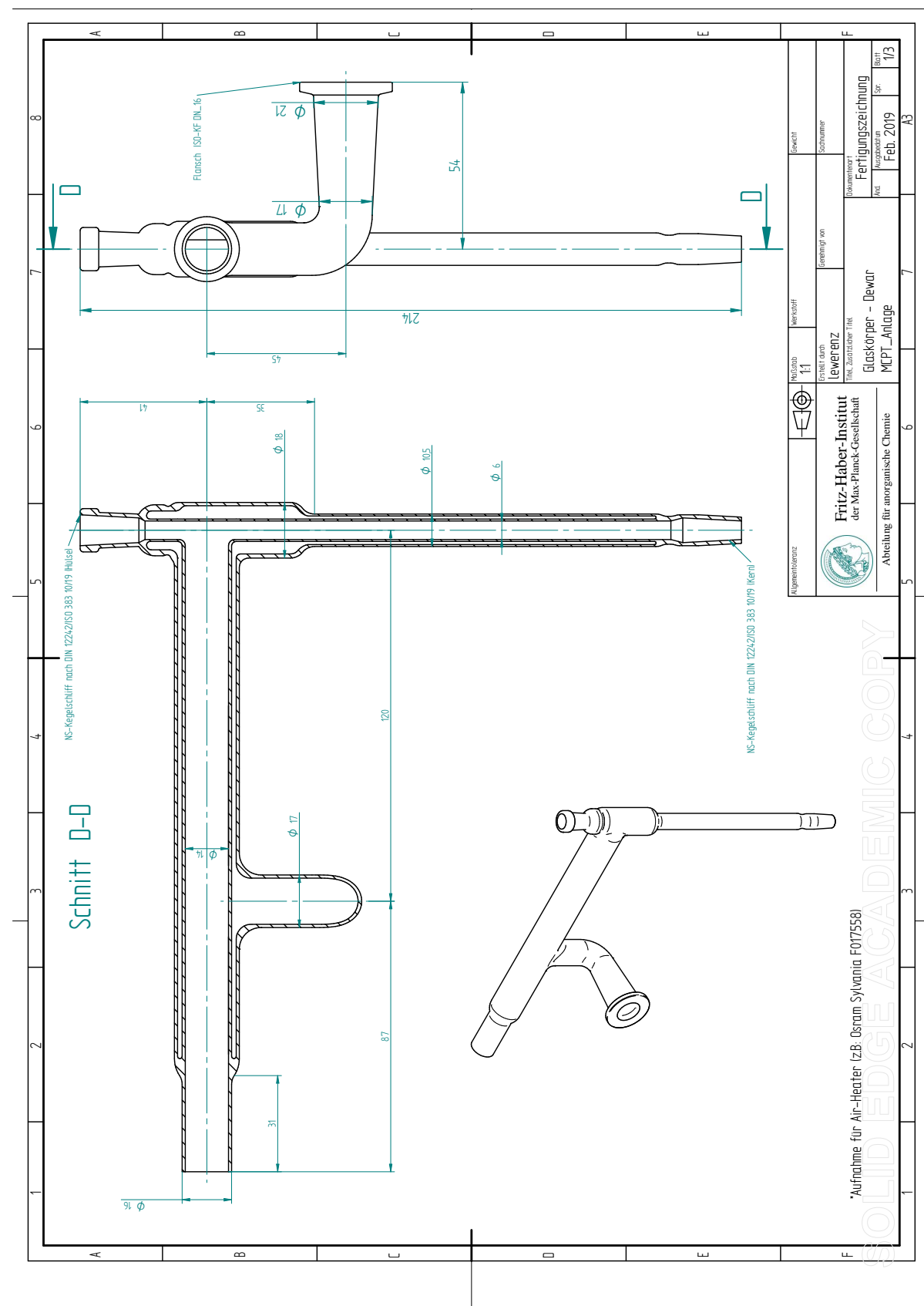


Figure S9: Heating jacket and vacuum dewar, made from HSQ100 (Quarzglas Heinrich, Aachen). Contains an opening for the air heater as well as a flanged connection for a vacuum pump.

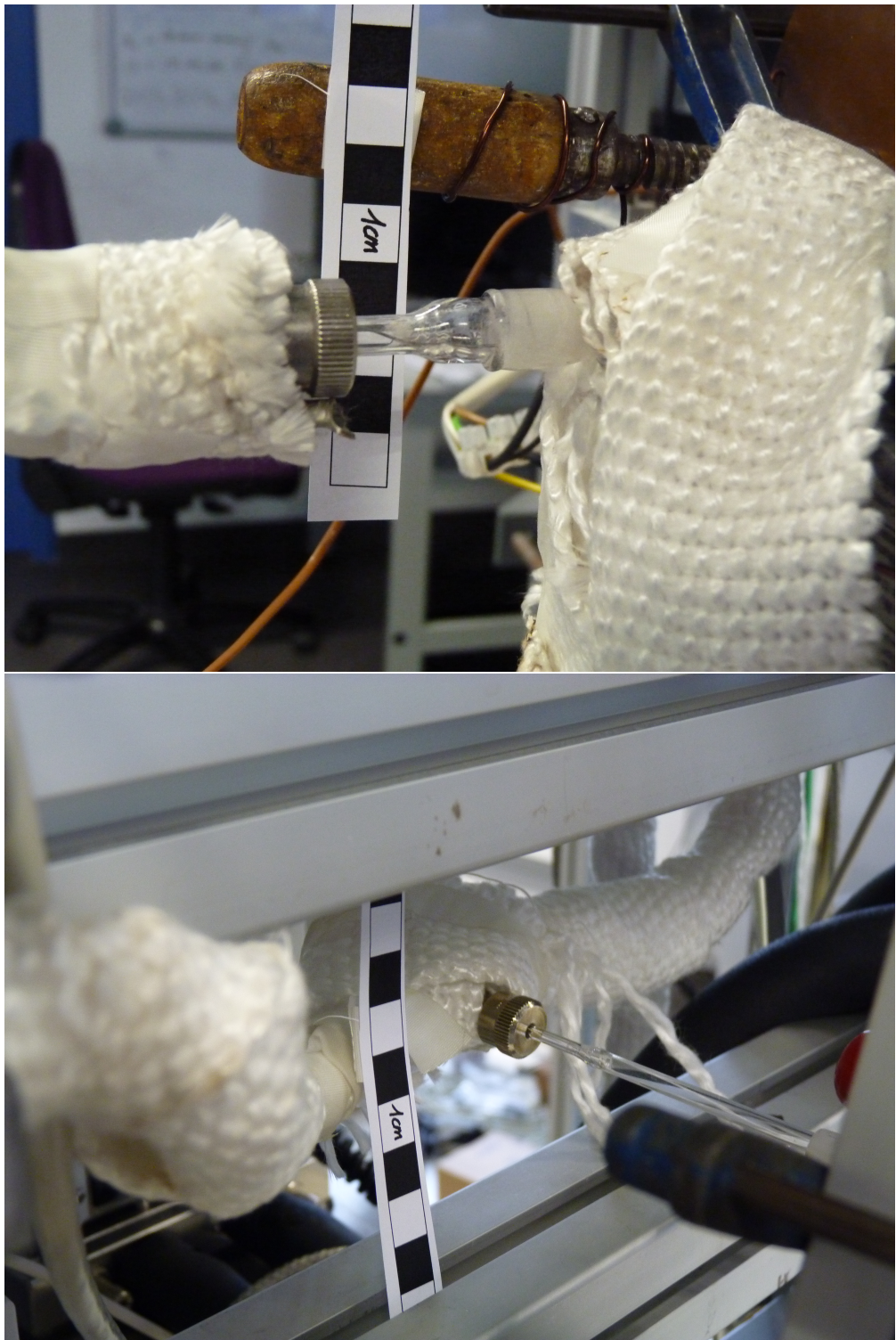


Figure S10: The connection at the inlet (top) and outlet (bottom) of the reactor, using Swagelok UltraTorr fittings.

Details of the temperature controller

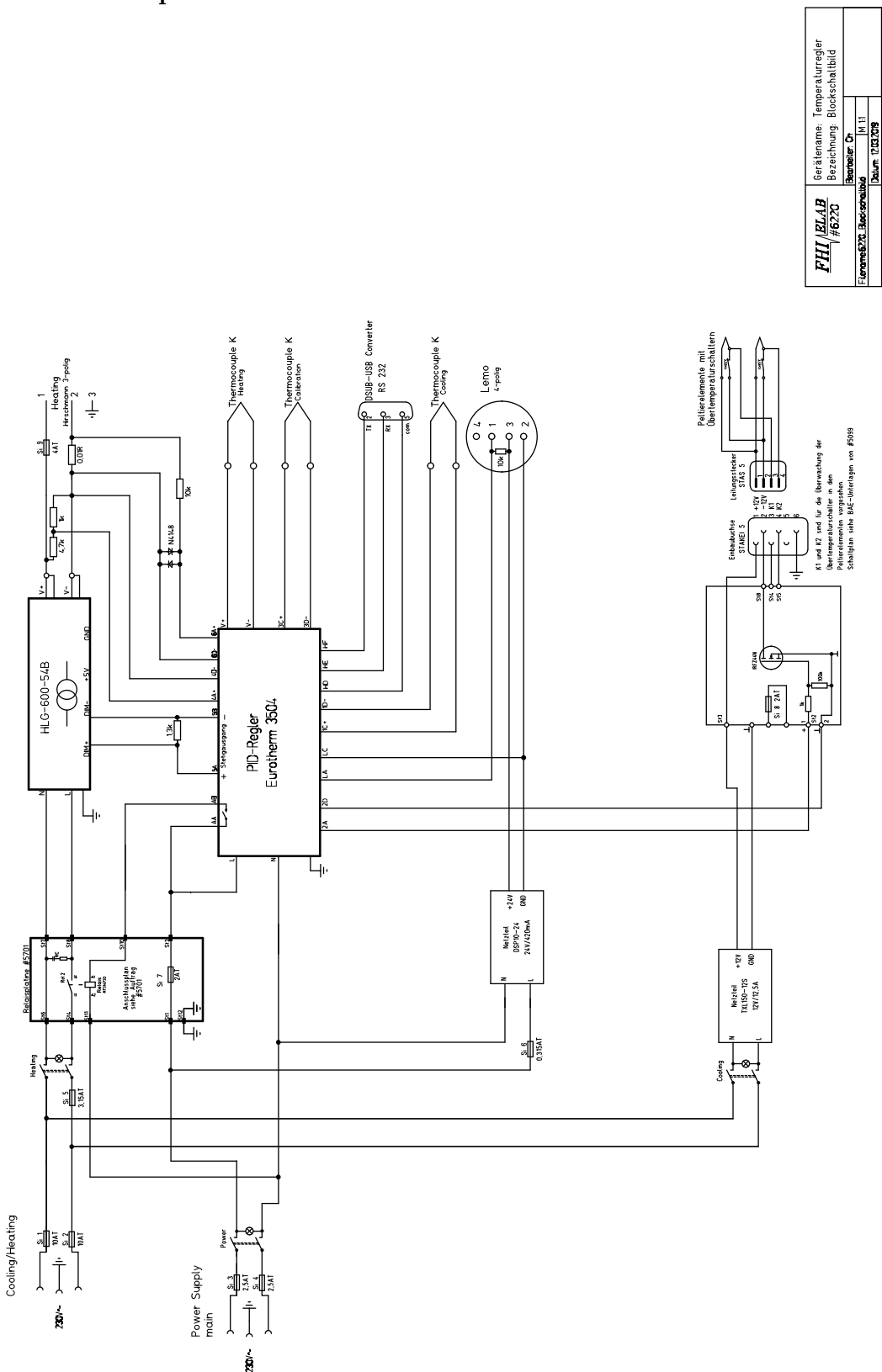


Figure S11: Wiring diagram of the temperature controller unit.



Figure S12: Front (top) and rear (bottom) view of the temperature controller unit.

Transmission line details

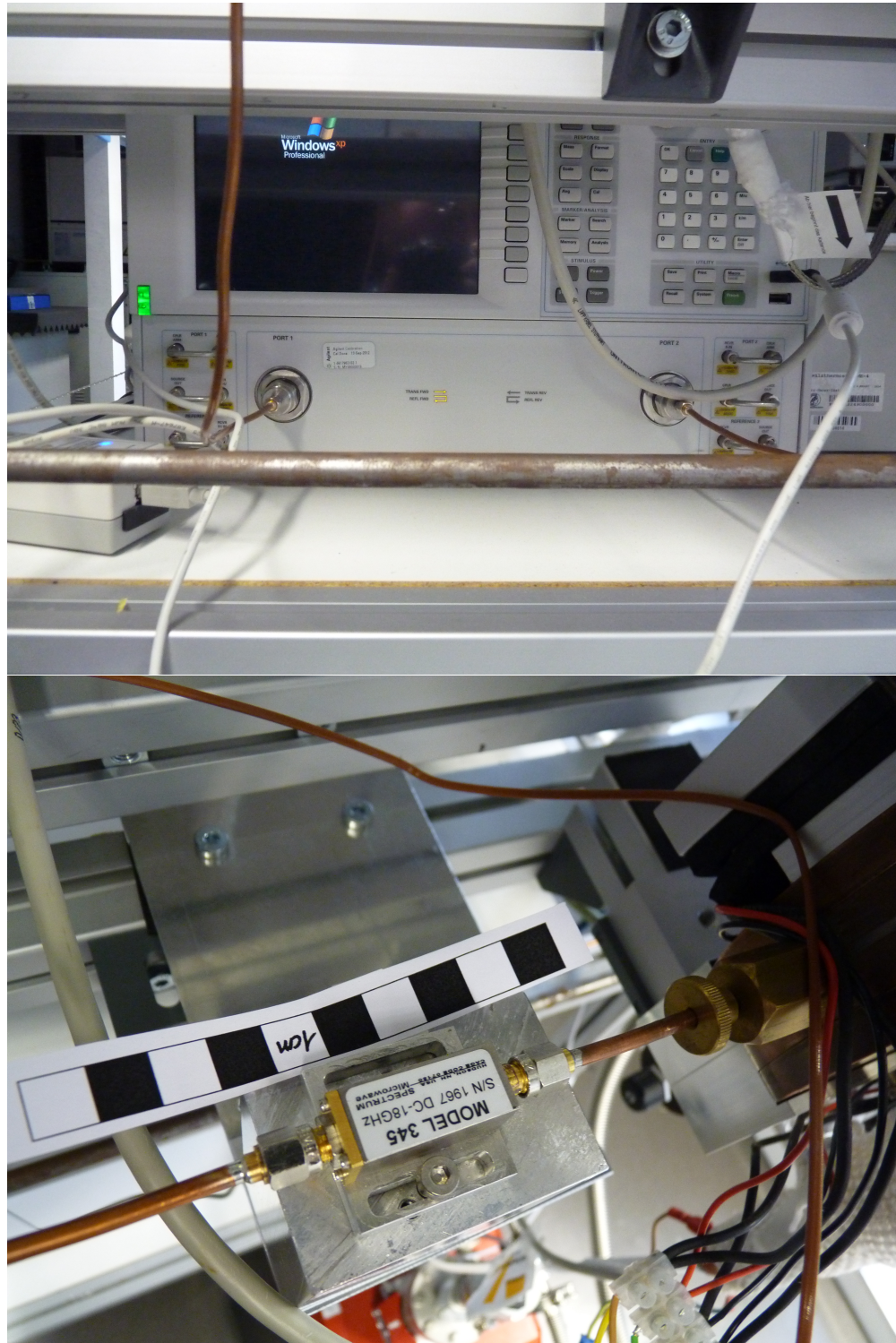


Figure S13: The coaxial transmission line leaving the network analyzer (top) and its connection to the cavity (bottom) via a filter and a coupling loop.